

Dynamical effects of phonons on soliton binding in spin-Peierls systems

D. Augier, D. Poilblanc, and E. Sørensen

Laboratoire de Physique Quantique and UMR CNRS 5626, Université Paul Sabatier, 31062 Toulouse, France

I. Affleck

Department of Physics and Astronomy, and Canadian Institute for Advanced Research, University of British Columbia, Vancouver, BC, Canada V6T 1Z1

(Received 9 June 1998)

The role of dynamical magnetoelastic coupling in spin-Peierls chains is investigated by numerical and analytical techniques. We show that a Heisenberg spin chain coupled to dynamical optical phonons exhibits a transition towards a spontaneously dimerized state in a wide range of parameter space. The low-energy excitations are characterized as solitons. No binding between solitons occurs in the isolated spin-phonon chain and the dynamical spin structure factor shows a broad magnon dispersion. However, elastic interchain coupling can lead to the formation of bound states. [S0163-1829(98)09438-7]

Quasi-one-dimensional (quasi-1D) magnetic systems have recently received renewed experimental and theoretical attention with the observation of the spin-Peierls transition in the two inorganic CuGeO_3 (Ref. 1) and NaV_2O_5 (Refs. 2–4) compounds which consist of weakly coupled spin- $\frac{1}{2}$ chains.⁵ While such a phenomenon was discovered in organic materials,⁶ the new inorganic compounds can be synthesized as relatively large single crystals allowing for new experimental studies.^{1–4,7–11}

The phase transition was inferred from an isotropic drop in the magnetic susceptibility¹ at a transition temperature T_{SP} signaling a nonmagnetic ground state (GS). The spin-Peierls transition is characterized by the opening of a spin gap, as has been observed by inelastic neutron scattering⁷ (INS) and NMR spectroscopy,^{8,3} accompanied by a distortion of the lattice observed in x-ray diffraction experiments.⁹

The formation at low temperature of a nonmagnetic GS has raised the possibility of observing topological magnetic excitations (solitons) as proposed theoretically in spin- $\frac{1}{2}$ frustrated Heisenberg spin chains¹² (the so-called J_1 - J_2 model, where J_1 and $J_2 = \alpha J_1$ are the nearest-neighbor and next-nearest-neighbor exchange couplings, respectively). At the Majumdar-Ghosh (MG) point, $\alpha = 0.5$, the GS is doubly degenerate corresponding to the two simple dimer patterns (called A and B) obtained by a regular succession of disconnected singlet (valence) bonds. In fact, for all $\alpha > \alpha_c$ ($\alpha_c \approx 0.241$),^{12–15} the GS was numerically shown to be dimerized. The elementary excitations in this phase are easily depicted at the MG point: a soliton s (antisoliton \bar{s}) consists of an unpaired spin separating two dimer patterns A (B) and B (A).¹⁶ These objects carry spin $\frac{1}{2}$ and can propagate thereby acquiring a dispersion. A spin-1 magnon excitation can be viewed as the excitation of a singlet bond into a triplet. However, in the J_1 - J_2 model, such excitations decay into unbound soliton and antisoliton excitations.

The spin-Peierls materials are widely described in the literature¹⁷ in terms of a static 1D antiferromagnetic frustrated dimerized Heisenberg chain¹⁸ which includes, in addition to the frustrating magnetic J_2 coupling, an explicit

dimerization δ of J_1 .¹⁹ Interchain interactions are neglected in this description. The values of J_1 and J_2 were estimated from a fit of the magnetic susceptibility at high temperature and the dimerization δ by requiring the model to have the experimental spin gap. Typical results such as $J_1 = 160$ K, $\alpha = 0.36$, $\delta = 0.014$ were obtained for CuGeO_3 (Refs. 20 and 14) and $J_1 = 440$ K, $\alpha = 0$, $\delta = 0.048$ for NaV_2O_5 (Refs. 4 and 21). The J_1 - J_2 - δ model successfully predicts^{22,23} the experimentally observed $s\bar{s}$ bound state.^{7,10} Indeed, the static potential of strength δ lifts the degeneracy between the two dimer A and B patterns. Therefore the energy cost of creating an A-B-A defect scales approximately as the length of the B structure. A confining force proportional to δ and to the separation between s and \bar{s} comes then naturally out.^{24–26} Besides the spin-1 magnons, this also suggests the existence of singlet $s\bar{s}$ bound states^{25,27,28} which could be seen, e.g., in Raman spectroscopy.¹¹

The static dimerized model has, nevertheless, some drawbacks. It shows no spontaneous symmetry breaking (since the dimerization is introduced *de facto* in the model) and ignores phonon dynamics which are expected to be important when the phonon frequency and the energy scale of spin fluctuations become comparable.

In this paper we investigate a *dynamical* spin-phonon model which fully incorporates the phonon dynamics. A weak-coupling renormalization-group (RG) treatment²⁹ is used to argue that this model spontaneously dimerizes even in the absence of interchain coupling (at $T=0$) for large enough spin-phonon coupling at all phonon frequency. Complementary numerical calculations are needed for arbitrary parameters and show that this spontaneous dimerization (accompanied by a simultaneous opening of a gap in the spin excitation spectrum) occurs in fact in a wide range of parameter space. The elementary excitations are characterized as solitons. We show the absence of $s\bar{s}$ binding for decoupled chains. However, in the presence of an elastic interchain coupling sharp spin-1 magnon excitations are recovered in the dynamical structure factor. Therefore we believe that a correct description of real materials must include the interchain coupling.³⁰

The key ingredient of the model is the magnetoelastic coupling; the exchange integral is *dynamically* modulated by the relative atomic displacements along the chains. Using independent phonon creation (destruction) operators b_i^\dagger (b_i) on each bond $(i, i+1)$ the model reads^{31,24}

$$H = J \sum_i \{ [1 + g(b_i + b_i^\dagger)] (\vec{S}_i \cdot \vec{S}_{i+1} - \frac{1}{4}) + \alpha (\vec{S}_i \cdot \vec{S}_{i+2} - \frac{1}{4}) \} \\ + H_{\text{ph}}^0 + H_{\perp},$$

where g is the magnetoelastic coupling constant. Here, we assume dispersionless optical phonons of frequency Ω , i.e., $H_{\text{ph}}^0 = \Omega \sum_i (b_i^\dagger b_i + \frac{1}{2})$. Presumably a model with on-site phonons will lead to similar results, however, the model used here is probably the more relevant to CuGeO₃.³² The inter-chain elastic coupling H_{\perp} will be discussed later.

The numerical results are based on Lanczos exact diagonalization³³ (ED) of closed rings with up to $L = 14$ sites supplemented by finite-size scaling analysis and a comparison with Bethe ansatz exact results of the Heisenberg chain and density matrix renormalization-group (DMRG) calculations of the frustrated J_1 - J_2 chain. A reliable treatment of the phonon dynamics is a difficult task. Preliminary studies have been carried out by considering a single $q = \pi$ phonon mode.³⁴ However, to investigate the *local* $s\bar{s}$ interaction it becomes necessary to consider the complete multimode problem.³⁵ We use here the variational treatment introduced by Fehrenbacher based on phononic coherent states. Two phononic states per site are retained including the vacuum and a phononic coherent state. This approach is nonperturbative, preserves the full dynamics of the phonons, and becomes exact in the weak- and strong-coupling limits.³⁶

As a first step, we shall consider the case of an isolated spin-phonon chain ($H_{\perp} = 0$). A RG argument similar to the one proposed in Ref. 29 can be used for this model for small $g^2\Omega/J$. Due to the SU(2) symmetry and the absence of charge excitations there is only one instantaneous interaction h , with a positive bare value, which is marginally irrelevant.²⁴ Integrating out the phonons generates a retarded electron-electron interaction \tilde{h} with a bare value $\tilde{h}(0) \approx -cg^2J/\Omega$ (c is a positive constant). One can then renormalize both types of interactions down to energies of the order of the phonon frequency. Below that scale, all interactions become essentially instantaneous leading to an effective Hamiltonian with new instantaneous interactions obtained by adding the retarded renormalized coupling $\tilde{h}(\Omega)$ to the instantaneous one $h(\Omega)$. The RG equations are²⁹ $h' = h^2$ and $\tilde{h}' = \frac{3}{2}h\tilde{h} + \tilde{h}^2$, involving the derivatives with respect to the logarithm of the energy scale. If the shift is large enough to change the sign of the instantaneous coupling [i.e., $h(\Omega) + \tilde{h}(\Omega) < 0$], the system is in the spontaneously dimerized phase. This scenario always occurs for a large enough coupling such that $cg^2 > \Omega h(0)/(2J)$ in the limit $\Omega \ll J$.

We now show numerically the existence of a $T = 0$ spontaneous symmetry breaking towards a dimerized phase in a

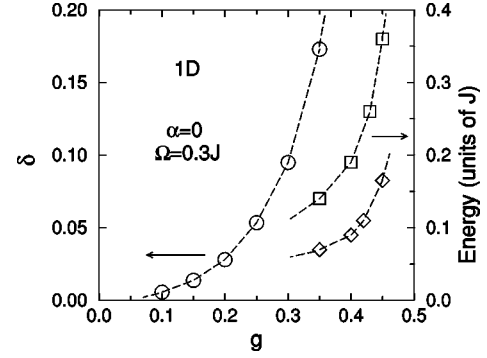


FIG. 1. Alternation in exchange integral δ^* (○), spin gap Δ^{01} (□), and soliton minimum energy Δ_S (◇) as a function of the coupling g for $\alpha=0$ and frequency $\Omega=0.3J$.

large region of parameter space. The dimerized phase is signaled, in the thermodynamic limit, by (i) the twofold degeneracy of the GS, (ii) the opening of a spin gap, and (iii) a lattice dimerization. The singlet-triplet spin gap $\Delta^{01}(L)$ as well as the separation $\Delta^{00}(L)$ between the singlet GS in the $K=0$ and $K=\pi$ momentum sectors were seen to scale accurately according to exponential laws.^{28,21} The data strongly suggest $\Delta^{00}=0$, evidence for a symmetry breaking in the GS. In addition, a finite extrapolated value of the spin gap Δ^{01} was obtained for a wide range of parameters. As shown in Fig. 1, Δ^{01} increases strongly with the magnetoelastic coupling g . Lower-frequency phonons were found even more effective in opening the spin gap.

Then, to gain more insight we have computed the structural distortion associated to the broken symmetry. The GS correlation function $C_{\text{latt}}(q) = \langle u_{-q} u_q \rangle_0$ of the Fourier components $u_q = L^{-1/2} \sum_i \exp(iqr_i) u_i$ of the relative lattice displacements ($u_i = b_i + b_i^\dagger$) exhibits a divergence at momentum $q = \pi$ of the form $C_{\text{latt}}(\pi) \propto L$. The dimerization δ^* of the exchange integral is defined by $\delta^{*2} = g^2 \lim_{L \rightarrow \infty} \{ L^{-1} C_{\text{latt}}(\pi) \}$. δ^* obtained from a finite-size scaling analysis is shown in Fig. 1 for $\alpha=0$ and $\Omega=0.3J$. Its g dependence follows closely the behavior of the spin gap. According to the previous RG analysis, δ^* should be nonzero above a critical coupling, which is consistent with numerical results.

We now turn to the characterization of the elementary magnetic excitations in the dimerized GS. If topological solitons exist in the spin-phonon model such excitations should be created in pairs. However, finite chains with an odd number of sites cannot accommodate a simple dimerized pattern and the GS of such a system is expected to contain a single solitonic excitation. Therefore, the energy difference defined by $E_S(k) = E_{\text{odd}}^0(L, k) - E_{\text{even}}^0(L)$, where $E_{\text{odd}}^0(L, k)$ is the GS energy of the chain of length $L = 2p + 1$ with momentum k and $E_{\text{even}}^0(L)$ is the absolute GS energy of even chains interpolated at $L = 2p + 1$, can be considered as the excitation energy of a spin- $\frac{1}{2}$ topological defect propagating with a momentum k along the chain. Note that, consequently soliton energies cannot be computed in models including an explicit translation symmetry breaking, like, e.g., the dimerized Heisenberg chain.³⁷ To test the accuracy of this procedure, we have compared our results for the spin-phonon model to the ones obtained for the purely magnetic J_1 - J_2 chain at the

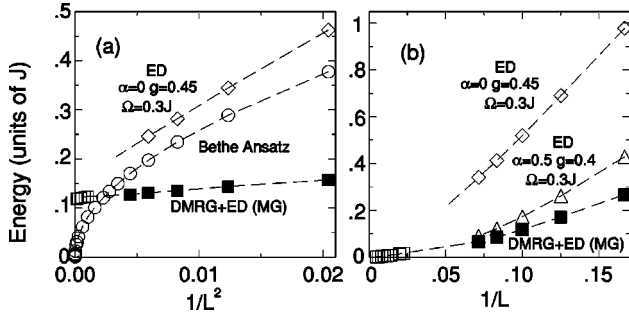


FIG. 2. (a) Minimum energy of the soliton E_S as a function of the inverse square of the chain length $1/L^2$ for $\alpha=0, g=0$ (\circ : Bethe ansatz), $\alpha=0.5, g=0$ (\square : DMRG, \blacksquare : ED), and $\alpha=0, g=0.45, \Omega=0.3J$ (\diamond , ED). (b) Binding energy E_B^{01} for $\alpha=0.5, g=0$ (\square : DMRG, \blacksquare : ED), $\alpha=0, g=0.45, \Omega=0.3J$ (\diamond), and $\alpha=0.5, g=0.4, \Omega=0.3J$ (\triangle) as a function of $1/L$.

MG point where the spin correlation length is the shortest. In both cases, ED of periodic chains show a dispersion which can be parametrized as $E_S(k) \approx \sqrt{\Delta_S^2 + v_S^2(k \mp \pi/2)^2}$, where Δ_S is the soliton gap and v_S a characteristic velocity. The lowest excitation in a finite system is then obtained for the momentum which is closest to $\pi/2$.³⁸ For the spin-phonon model, Δ_S appears to be finite for a wide region of parameter space [see Fig. 2(a)]. Hence, the spin- $\frac{1}{2}$ excitation spectrum is massive indicating the existence of solitons contrary to the case of the Heisenberg chain where spin- $\frac{1}{2}$ excitations (called spinons) are gapless,³⁹ as explicitly shown in Fig. 2(a) using the Bethe ansatz solution for $\alpha=0$.⁴⁰ The soliton gap should not depend on boundary conditions, and using DMRG data for open chains,³⁸ we estimate $\Delta_S \approx 0.1170(2)J$ at the MG point in the absence of a spin-phonon coupling in good agreement with the estimate in Ref. 16 of $\Delta_S \approx 0.125J$.

Spin-1 magnons can be considered as a $s\bar{s}$ combination in a triplet state. Consequently, the excitation triplet and *second* singlet gaps are written as $\Delta^{ab} \approx 2\Delta_S + E_B^{ab}$, where E_B^{ab} accounts for a finite-range spin-dependent interaction between s and \bar{s} . E_B^{ab} is finite only if the $s\bar{s}$ combination forms a bound state; otherwise it vanishes and s and \bar{s} separate to infinity. The latter scenario occurs, for example, in the spontaneously ($\alpha > \alpha_c$) dimerized frustrated Heisenberg chain²⁴ where $\Delta^{00} = \Delta^{01}$. However, in the case of spin-phonon models, a direct comparison between Δ^{00} and Δ^{01} requires some caution: low-energy spin-0 excitations of phononic character are likely to exist and are indistinguishable from the magnetic singlet $s\bar{s}$ excitations. The triplet binding energy $E_B^{01} = \Delta^{01} - 2\Delta_S$ can nevertheless be calculated on closed rings and ED results are shown in Fig. 2(b). The data for the spin-phonon model are very similar to the DMRG data on open chains at the MG point [also shown in Fig. 2(b)] strongly suggesting a vanishing binding energy for all parameters. This is consistent with the weak-coupling RG treatment: one obtains an effective field theory similar to the one describing the pure spin system (with renormalized coupling constants) and no bound state is expected.²⁴ We conclude that solitons and antisolitons are not bound in the 1D spin-phonon model.

Because of the decay of the $s\bar{s}$ pair, we do not expect any

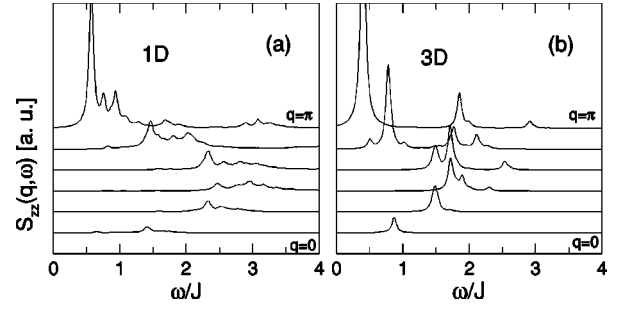


FIG. 3. Dynamical spin factor structure $S_{zz}(q, \omega)$ calculated at momenta $q = 2\pi n/L$, $n = 0, \dots, L/2$ ($L = 12$) (a) for $\alpha=0, g=0.3, \Omega=0.2J$ and no interchain coupling; (b) for $\alpha=0, g=0.08, \Omega=0.2J$, and $\lambda=0.1J$. High-energy peaks are due to finite-size effects. A small broadening $\varepsilon=0.04J$ was used.

sharp δ -function structure in the low-frequency spin structure factor. The latter which can be experimentally obtained by INS is defined as $S_{zz}(q, \omega) = \sum_n |\langle \Phi_n | S_z(q) | \Phi_0 \rangle|^2 \delta(\omega - E_n + E_0)$, where E_0 (E_n) is (are) the energy(ies) of the GS Φ_0 (triplet states Φ_n) and $S_z(q)$ is the Fourier transform of S_z^i . Results for the spin-phonon model on a 12-site chain are shown in Fig. 3(a) for realistic parameters of NaV_2O_5 (i.e., leading to a spin gap $\Delta^{01} \approx 0.2J$) and are strikingly different from those obtained for a static dimerization.²¹ The main structure, although reminiscent of the well-known spinon dispersion of the Heisenberg chain [$\omega(q) = (\pi/2)J|\sin q|$],³⁹ is shifted towards higher energies and is much broader. Furthermore, the relative weight of the low-energy peak (e.g., at $q = \pi/2$) decreases for increasing system size. Consistent with the previous analysis, there are no well-defined spin-1 magnons.

Next, we argue that the interchain coupling is crucial in order to produce well-defined magnon excitations as experimentally observed. To test this scenario we have considered an elastic interchain coupling of the form,²⁴ $H_\perp = K_\perp \sum_i \sum_{\langle \gamma, \gamma' \rangle} u_i^\gamma u_i^{\gamma'}$, where $\langle \gamma, \gamma' \rangle$ refers to adjacent chains. We shall treat this interchain elastic coupling at the mean-field level,^{31,24} while retaining the full dynamics of the 1D phonons. A given chain γ will then be elastically coupled to the static deformation $\langle u_i^\gamma \rangle_0 = (-1)^i u_0$ of the Z neighboring chains. Consequently we get an additional *dynamical* term, $H_{\perp, \text{MF}} = \lambda \sum_i (-1)^i (b_i + b_i^\dagger)$ where $\lambda = ZK_\perp u_0$, which explicitly doubles the unit cell.

Turning on a small mean-field interchain coupling λ in the absence of frustration could again favor one of the two lattice distortions and confine solitons into pairs, in which case a number of $s\bar{s}$ stable bound states proportional to $1/\lambda$ (in the limit $\lambda \ll J$) would be expected.²⁴ Although the previous analysis on soliton binding cannot be done anymore, we give further arguments in favor of soliton binding based on the study of the dynamical structure factor. This one is shown on Fig. 3(b) for parameters relevant to NaV_2O_5 with a nonzero value of λ . Qualitatively, the low-energy magnon structure is now much better defined and the magnon dispersion is clearly apparent. The maximum of the dispersion occurs at $\omega \approx 1.7J$, an energy close to the exact value $(\pi/2)J$ of the Heisenberg chain.³⁹ At momentum $q = \pi/2$ where

finite-size effects are shown to be quite small,^{23,21} the average frequency $\langle\omega\rangle$ and the width $\Delta\omega$ of the structure depend strongly on the presence of an interchain coupling. The structure clearly gets narrower when the interchain coupling increases. Furthermore, when $\lambda \neq 0$ the relative weight of the

lowest-energy peak increases with the length of the chain, contrary to the case of the isolated chain.

We thank IDRIS (Orsay) for allocation of CPU time on the C94 and C98 CRAY supercomputers. The research of I.A. was supported in part by NSERC of Canada.

-
- ¹M. Hase, I. Terasaki, and K. Uchinokura, Phys. Rev. Lett. **70**, 3651 (1993).
²M. Isobe and Y. Ueda, J. Phys. Soc. Jpn. **65**, 1178 (1996).
³T. Ohama *et al.*, J. Phys. Soc. Jpn. **66**, 545 (1997).
⁴M. Weiden *et al.*, Z. Phys. B **103**, 1 (1997).
⁵See, e.g., H. Horsch and F. Mack, cond-mat/9801316 (unpublished) for the case of NaV₂O₅.
⁶See J. W. Bray *et al.*, in *Extended Linear Chain Compounds*, edited by J. S. Miller (Plenum Press, New York, 1983), Vol. 3.
⁷L. P. Regnault *et al.*, Phys. Rev. B **53**, 5579 (1996).
⁸M. Itoh *et al.*, Phys. Rev. B **53**, 11 606 (1996).
⁹J. P. Pouget *et al.*, Phys. Rev. Lett. **72**, 4037 (1994); Y. Fujii *et al.*, J. Phys. Soc. Jpn. **66**, 326 (1997).
¹⁰M. Aïn *et al.*, Phys. Rev. Lett. **78**, 1560 (1997).
¹¹P. van Loosdrecht *et al.*, Phys. Rev. Lett. **76**, 311 (1996); P. van Loosdrecht, cond-mat/9711091 (unpublished); S. A. Golubchik *et al.*, J. Phys. Soc. Jpn. **66**, 4042 (1997).
¹²F. D. M. Haldane, Phys. Rev. B **25**, 4925 (1982).
¹³K. Okamoto and K. Nomura, Phys. Lett. A **169**, 433 (1992); R. Chitra *et al.*, Phys. Rev. B **52**, 6581 (1995).
¹⁴G. Castilla, S. Chakravarty, and V. J. Emery, Phys. Rev. Lett. **75**, 1823 (1995).
¹⁵S. R. White and I. Affleck, Phys. Rev. B **54**, 9862 (1996).
¹⁶B. Shastri and B. Sutherland, Phys. Rev. Lett. **47**, 964 (1981).
¹⁷For a review, see, e.g., J. P. Boucher and L. P. Regnault, J. Phys. I **6**, 1939 (1996).
¹⁸E. H. Lieb and B. Nachtergaele, Phys. Rev. B **51**, 4777 (1995).
¹⁹E. Pytte, Phys. Rev. B **10**, 4637 (1974); M. C. Cross and D. S. Fisher, Phys. Rev. B **19**, 402 (1979).
²⁰J. Riera and A. Dobry, Phys. Rev. B **51**, 16 098 (1995).
²¹D. Augier *et al.*, Phys. Rev. B **56**, R5732 (1997).
²²A. Fledderjohann and C. Gros, Europhys. Lett. **37**, 189 (1997).
²³D. Poilblanc *et al.*, Phys. Rev. B **55**, R11 941 (1997).
²⁴I. Affleck, Proceedings of the NATO ASI: Dynamical properties of Unconventional Magnetic Systems, April, 1997, cond-mat/9705127 (unpublished).
²⁵G. Uhrig and H. Schulz, Phys. Rev. B **54**, R9624 (1996).
²⁶R. Werner and C. Gros, Phys. Rev. B **57**, 2897 (1998).
²⁷V. N. Nuthukumar *et al.*, Phys. Rev. B **54**, R9635 (1996).
²⁸G. Bouzerar, A. P. Kampf, and F. Schönfeld, cond-mat/9701176 (unpublished).
²⁹G. T. Zimanyi, S. A. Kivelson, and A. Luther, Phys. Rev. Lett. **60**, 2089 (1988); L. Caron and C. Bourbonnais, Phys. Rev. B **29**, 4230 (1984).
³⁰G. S. Uhrig, Phys. Rev. Lett. **79**, 163 (1997).
³¹D. Khomskii, W. Geerstma, and M. Mostovoy, Czech. J. Phys. **46**, Suppl S6, 32 (1996).
³²W. Geerstma and D. Khomskii, Phys. Rev. B **54**, 3011 (1996).
³³D. Poilblanc, in *Numerical Methods for Strongly Correlated Systems*, edited by D. J. Scalapino (Frontiers in Physics, Redwood City, CA, 1997); E. Dagotto, Rev. Mod. Phys. **66**, 763 (1994).
³⁴D. Augier and D. Poilblanc, Eur. Phys. J. B **1**, 19 (1998).
³⁵See A. W. Sandvik, R. R. P. Singh, and D. K. Campbell, Phys. Rev. B **56**, 14 510 (1997) for a QMC approach.
³⁶The method was shown to be also accurate in the intermediate range: R. Fehrenbacher, Phys. Rev. B **49**, 12 230 (1994); Phys. Rev. Lett. **77**, 2288 (1996).
³⁷The occurrence of bound states in the dimerized Heisenberg chain can nevertheless be discussed using a different approach. See, e.g., E. Sørensen *et al.*, cond-mat/9805386 (unpublished).
³⁸If $\Delta_S \neq 0$, one expects $1/L^2$ corrections in the energy.
³⁹J. Des Cloiseaux and J. J. Pearson, Phys. Rev. **128**, 2131 (1962).
⁴⁰In this case, $E_S \propto 1/L$ (with logarithmic corrections).